

Contents lists available at ScienceDirect

Climate Change Ecology

journal homepage: www.elsevier.com/locate/ecochg



A Late-Holocene palynological record of coastal ecological change and climate variability from Apalachicola, Florida, U.S.A



Qiang Yao^a, Erika Rodrigues^{a,b,*}, Kam-biu Liu^a, Caitlin Snyder^c, Nicholas Culligan^a

- ^a Department of Oceanography and Coastal Sciences, College of the Coast and Environment, Louisiana State University, Rm 3280, 93 South Quad Drive, Baton Rouge, LA 70803, USA
- ^b Graduate Program of Geology and Geochemistry, Federal University of Pará, Av. Perimentral 2651, Terra Firme, Belém, PA 66077-530, Brazil
- ^c Apalachicola National Estuarine Research Reserve, Eastpoint, FL 32328, USA

ARTICLE INFO

Keywords: Mangrove expansion Global warming Sea-level rise Palynology Multi-proxy analysis

ABSTRACT

This study uses radiometric dating, palynological, loss-on-ignition, and X-ray fluorescence analyses to reconstruct the vegetation history and coastal morphological changes at the boreal mangrove range limit along the Gulf of Mexico, based on three sediment cores taken from St. George Island, Apalachicola, Florida, USA. The multi-proxy record indicates that the mangrove stands in the vicinity of St. George Island were formed in the recent decades, and no signs of mangroves were found for the last 1500 years during the Late-Holocene in the sedimentary record. The current mangrove expansion at St. George Island is caused by the recent climate warming instead of a recurring phenomenon tied with cyclical global climate variability. Further analysis based on decadal-scale climatic and environmental records reveal that the accelerated sea-level rise and warmer winters, especially the decrease of winter freeze events in the 21st century, are the most plausible causes for mangrove expansion at their boreal range limit during the recent decades. Under the predicted warming trend and accelerating sea-level rise in the 21st century, it is reasonable to believe that mangrove encroachment into coastal marshes will accelerate at Apalachicola and other areas near their poleward range limits.

1. Introduction

Mangroves are one of the most productive foundation species in the tropics and subtropics that provide essential ecosystem services [12,35], including but not limited to storm protection [2], natural life nursery [11], and carbon sequestration [43]. They also grow in similar latitudes and terrains with another foundation species – coastal marsh. Since the early 21st century, substantial mangrove encroachment into coastal marshes has been observed along the U.S Gulf of Mexico (GOM) coast-lines due to global warming [8,25,5,33]. Under the projected warming trend in the 21st century (IPCC, 2021), many studies have suggested that a much more aggressive mangrove encroachment will occur in the GOM states in the near future [50,52,5,32,37]. The zonation shifts of these foundation species will significantly alter the aforementioned ecosystem functions and services and impact the local fauna and flora [17,19]. Thus, there is an urgent need to monitor the mangrove dynamics and understand the driving mechanisms that control their range.

In the continental United States, only three true mangrove species are found: *Avicennia germinans* (black mangrove), *Rhizophora mangle* (red mangrove), and *Laguncularia racemosa* (white mangrove). The main

mangrove habitats are located in Louisiana and Florida, with R. mangle confined to southernmost Texas and only scattered black mangrove populations in Texas [28,29] (Fig. 1). In particular, the mangrove populations along the northern GOM coastlines are reaching their poleward range limit in the Northern Hemisphere [1] where they are very sensitive to climate variations [4,14]. Historically, Cedar Keys in Florida was considered the poleward mangrove range limit in the continental U.S [20]. However, more and more individuals of black and red mangroves have been spotted in Apalachicola (~200 km to the northwest of Cedar Keys), and a few populated mangrove stands have formed in the area in recent years (Fig. 1) [40]. Such mangrove "tropicalization" has drawn attention from ecologists and biologists from across the U.S [52,5,32]. However, most remote sensing and ecological studies can only provide a decadal-scale record, and very few studies have documented the longterm ecological changes and climate variabilities at this new mangrove frontier. Hence, it is still unclear whether the mangrove encroachment in Apalachicola is a recurring phenomenon tied to long-term global climate variability or caused by the recent climate changes.

To fill these data gaps, this study utilizes the time-tested methods – palynology, radiometric dating, loss-on ignition (LOI), and X-ray fluores-

E-mail address: erikarodrigues@ufpa.br (E. Rodrigues).

^{*} Corresponding author at: Department of Oceanography and Coastal Sciences, College of the Coast and Environment, Louisiana State University, Rm 3280, 93 South Quad Drive, Baton Rouge, LA 70803, USA.

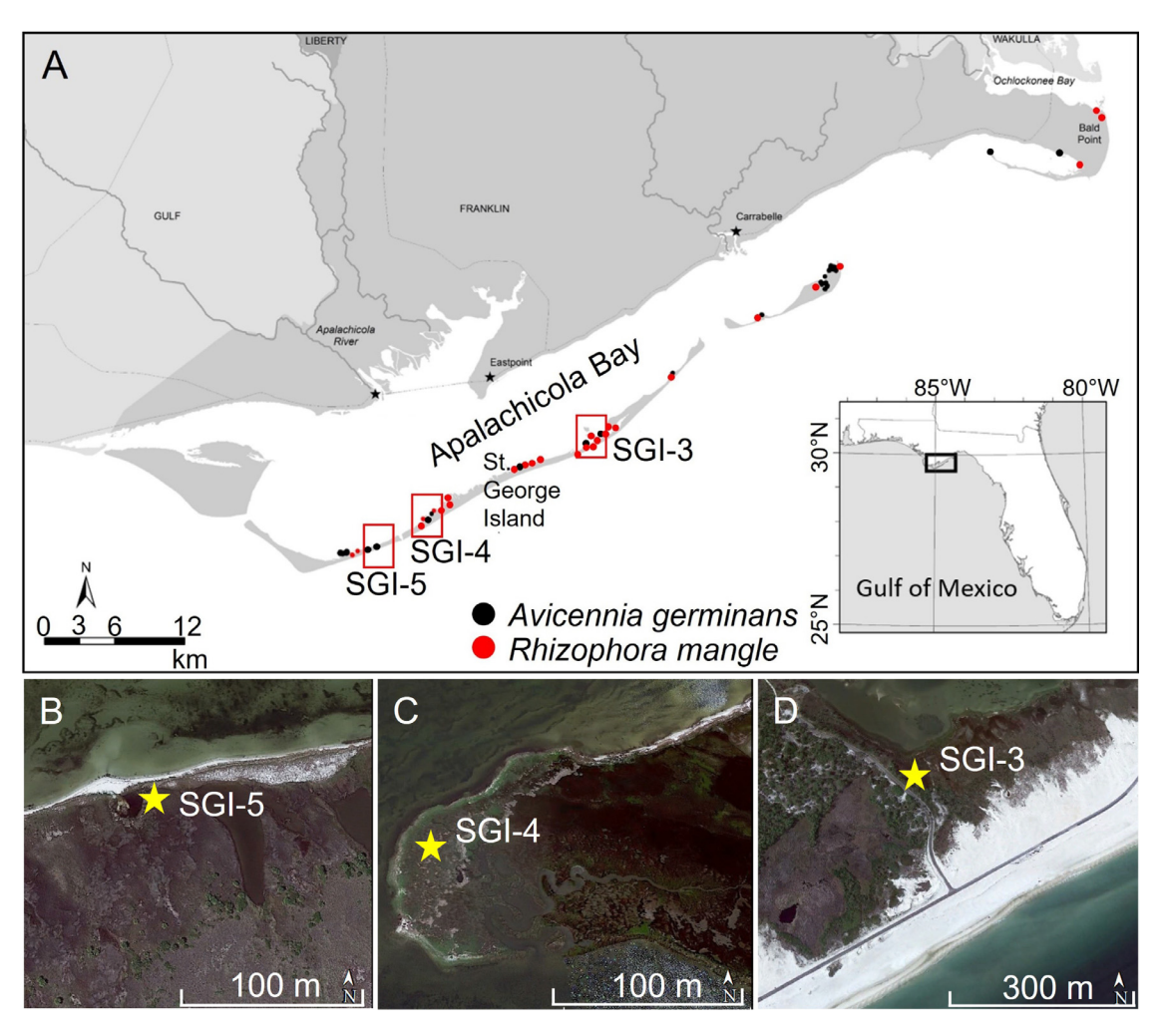


Fig. 1. Maps showing the study area (A) and coring locations (yellow star) of SGI-5 (B), SGI-4 (C), and SGI-3 (D). The black and red dots mark the distribution of A. germinans and R. mangle in the study area, respectively.

cence (XRF) analyses on three sediment cores (SGI-3,4,5) to reconstruct the vegetation dynamics and coastal geomorphological development in Apalachicola for the last 1500 years (Fig. 1). We also compare the proxy data with a 31-year (1990–2020) record of temperature, precipitation, and relative sea-level (RSL) changes from Apalachicola to reveal the driving factors behind vegetation dynamics at this new mangrove frontier in the light of climate changes. The overarching objectives of this study are to investigate the following research questions: (1) Did mangroves establish in Apalachicola prior to the industrial-era, especially during the Late-Holocene? (2) What are the potential causes for poleward mangrove migration, from the perspectives of the paleoecological record?

2. Materials and methods

2.1. Study site description

Apalachicola currently marks the northernmost distribution of both *A. germinans* and *R. mangle* along the northern GOM. According to historical documents, mangroves have been spotted near the Apalachicola Bay for ~150 years, but more and more mangroves have been sighted since the early 21st century [49,40]. Our study area - St. George Island is comprised of 50–100 m wide white sand beach on the gulf side. Behind the beach are sand dunes at ~2–10 m tall. Shrubs (e.g., Ericaceae and *Myrica*), graminoids (*Juncus roemerianus* and *Spartina alterniflora*), and succulent plants (*Batis maritima* and *Salicornia perennis*) can be found on

the newer dunes, and pine savanna (e.g., *Pinus* and *Quercus*) occupies the older relic dunes (Fig. 2) [45]. Currently, several robust mangrove stands are found on the bayside of the St. George Island (Figs. 1, 2), particularly near St. George Park where the longest core – SGI-3 was taken (Fig. S1 in Supplementary Content). The mangrove individual size and colony have both increased since they were first observed in 2004 [40]. Salt marshes near the Apalachicola Bay are primarily occupied by sedge/reed at lower intertidal elevations, and dune vegetation in higher elevations. Clearly these marsh systems represent suitable habitats for the advancing populations of both *A. germinans* and *R. mangle* to invade and colonize under a warmer climate [40]. However, it remains to be demonstrated if and how such a small pioneer population of mangroves is registered palynologically in the modern pollen record. It is also unknown whether one, or both, species of mangroves was present here during the Late-Holocene.

2.2. Sampling and lithological description

Ground and aerial surveys using a DJI Phantom 4 Advanced drone equipped with GPS, inertial measurement, and digital 4 K/20MP (RGB) camera (spatial resolution of 1.6 cm/pixel at 60 m) were conducted to identify the locations of mangrove stands and other vegetation units prior to coring (Figs. 2, S1). Three sediment cores (SGI-3 – 220 cm, 29°41′29.94″N/84°47′8.16″W; SGI-4 – 90 cm, 29°38′49.86″N/84°55′17.94″W, and SGI-5 – 40 cm, 29°36′24.78″N /84°59′21.24″W) were acquired via a vibra-corer near the three largest



Fig. 2. Photos of the main vegetation units on St. George Island - pine savanna (a), mangroves (b), and beach vegetation (c).

Table 1Radiocarbon dating results for sedimentary cores.

SAMPLE ID	SAMPLE TYPE	CONVENTIONAL AGE(BP)	CALIBRATED AGE (cal yr BP)	2-SIGMA CALIBRATION (cal yr BP)
SGI-3 49-50 cm	Organic Sediment	660 +/- 40	620	554 - 613 (50.6%)\$\$\$\$622 - 672 (49.4%)
SGI-3 100 cm	Organic Sediment	690 +/- 30	670	562 - 590 (31.5%)\$\$\$\$632 - 677 (68.5%)
SGI-3 215 cm	Organic Sediment	1630 +/- 30	1490	1409 - 1550 (97%)\$\$\$\$1552 - 1569 (3%)
SGI-4 25 cm	Organic Sediment	Modern	Modern	N/A
SGI-4 80 cm	Organic Sediment	740 +/- 30	680	653 – 724 (100%)
SGI-5 39 cm	Organic Sediment	Modern	Modern	N/A

mangrove stands on the bayside of the St. George Island (Fig. 1). All cores have reached the bottom hard substrate and contained a complete sedimentary history at the coring locations. The cores were measured, photographed, and wrapped in the field and are currently stored in the Global Change and Coastal Paleoecology Laboratory in Louisiana State University. Sedimentary features such as color and texture were used to characterize the lithology [18,46]. The pollen, LOI, and XRF datasets were grouped into facies associations to determine the ecological and morphological changes.

2.3. Chronology

Six samples consisting of treated bulk organic sediments and plant tissues were sent to ICA Inc., Sunrise, FL for Accelerator Mass Spectrometry (AMS) ¹⁴C dating (Table 1). Samples were pre-treated following the analytical procedures described in Yao et al., [50]. All radiocarbon dating results were calibrated by using Calib 8.2 [41], converted to calibrated year before present (cal yr BP), and rounded to the nearest decade.

2.4. XRF and LOI analyses

X-ray fluorescence (XRF) and Loss-on-ignition (LOI) analyses were performed at a continuous 1-cm interval on all three cores. XRF can measure the concentration (ppm) of major chemical elements in coastal

sediments (e.g., Ca, Ti, and Br) and is commonly used in sedimentary studies ([53,55], 2021). Among the XRF data curves, Ca/Ti and Cl/Br ratios showed the most significant and meaningful variabilities and are therefore displayed in this study. LOI analysis was performed by heating the sediment samples at 105°, 550°, and 1000 °C to measure the water (wet weight), organic (dry weight), and carbonate (dry weight) contents, respectively [22].

2.5. Palynological analysis

Cores SGI-3 and SGI-4 were sampled at 5-cm intervals, and core SGI-5 was sampled at 10-cm intervals. For each sample, approximately 1 ${\rm cm}^3$ of sediment was used for pollen analysis. One tablet of Lycopodium spores containing 20,848 grains was added to each sample as an exotic marker to aid the calculation of pollen concentration (grains/cm³) following the formula: Pollen concentration = $P_c * L_a / L_c * V$.

Where P_c is the number of fossil pollen counted, L_a is the number of *Lycopodium* spores added (20,848), L_c is the number of *Lycopodium* spores counted, and V is the volume of the sample. Pollen samples were treated following the conventional analytical procedure described in Yao et al., [50]. Published pollen keys by Yao and Liu [51] and Willard et al. [48] were used as references. Approximately 300 grains of pollen and spores were counted for each sample, except for the ones that were marked as "Pollen poor" in SGI-3&4, by using an Olympus microscope at $400 \times$ magnification. In addition, foraminifera linings and dinoflagel-

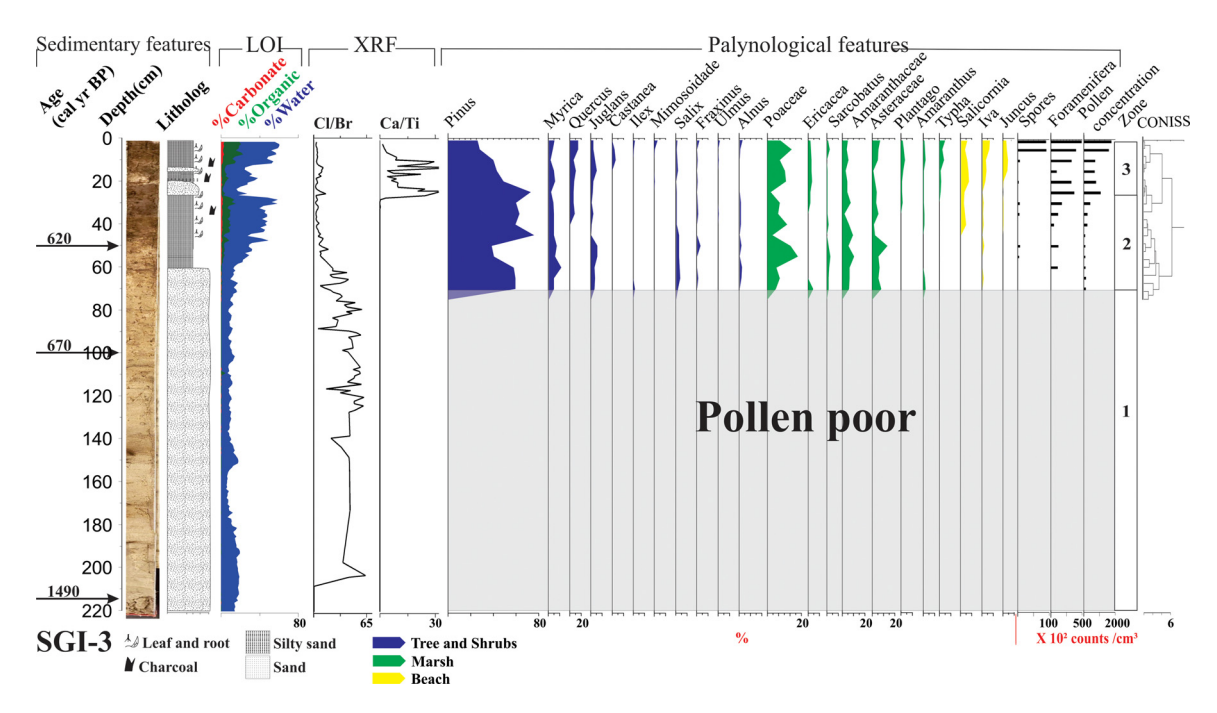


Fig. 3. Multi-proxy results of core SGI-3. Samples from 220 to 70 cm contain less than 50 grains of pollen and non-pollen palynomorphs in total and are marked as "Pollen poor".

late tests were also counted but not included in the total pollen sum and concentration. Cluster analysis dendrograms and pollen diagrams were plotted by using TILIA (v.1.7.16) [15]. The pollen taxa were categorized into trees and shrubs, marsh, and beach groups.

2.6. Environmental data collection and analysis

To determine the long-term environmental and climatic trends of our study area, we acquired daily temperature (1992-2019) and precipitation (1992–2019) data from the meteorological station (USW00012832) near Apalachicola, FL from US Climate Data (USCD) database (https://www.usclimatedata.com/climate/united-states/us). Sea-level data (1990-2020) were retrieved from Apalachicola (#8,728,690) meteorological station from National Oceanic and Atmospheric Administration, Center for Operational Oceanographic Products and Services (NOAA CO-OPS) (https://tidesandcurrents.noaa.gov/sltrends/). Since mangroves are tropical/subtropical plants and their range is believed to be limited by cold temperature [33], only winter temperature trends were discussed in this study. Thus, four metrics were calculated based on the daily dataset, which are winter (Dec to Feb) daily minimum air temperature (WDMAT), winter monthly average air temperature (WMAAT), monthly accumulated precipitation (MAP), and annual rates of sea level rise. Since mangroves were first observed from the study area between 2004 and 2009 and have been expanding continuously since then (Snyder et al., 2019), we use 2005 as the median (1990-2020) to split the dataset into the earlier and recent halves to compare the trends of these metrics and infer the possibly driving factors for mangrove encroachment in our study area. Regression analysis was developed using the R package "IM Function" (R [34]).

3. Results

3.1. Chronology and lithology

Radiocarbon dating results are presented in Table 1. The recorded ages ranged from modern to 1490 cal yr BP. Core SGI-3 (220 cm) is the longest among all three cores and consists of silty sand (0–30 cm) and sand (30–40 cm). The bottom age of core SGI-3 is determined to

be ~1500 cal yr BP and the majority of the core is comprised of sand (60-220 cm). Above the sand section is 60 cm of slightly finer silty sand containing abundant plant detritus (Fig. 3). Two radiocarbon dates obtained at 50 and 100 cm from the upper part of the core were calibrated to ~620 and 670 cal yr BP. Hence, the transition between sand and silty sand section is ~ 630 cal yr BP. Core SGI-4 consists of three types of sediments - peaty silt (0-25 cm), silty sand (25-70 cm), and sand (70-90 cm) (Fig. 4). The radiocarbon date obtained from 80 cm near the bottom of the core is calibrated to ~ 680 cal yr BP, suggesting that the bottom age of the core is ~ 800 cal yr BP. The radiocarbon sample obtained from 25 cm is dated to be modern, suggesting that the transition between peaty silt and silty sand section occurred after the 1950s (using AD 1950 as 0 cal yr BP). Core SGI-5 (40 cm) is the shortest among all three cores and consists of silty sand (0-30 cm) and sand (30-40 cm). The bottom age of this core is determined to be modern, suggesting that the entire sediment profile collected from this location was deposited after the 1950s (Fig. 5).

3.2. Sedimentary and geochemical characteristics

The LOI and XRF analyses and visual inspection revealed that core SGI-3 (220 cm, >1490 cal yr BP) exhibit two types of sedimentological environment (Fig. 3). The bulk of the core consists of sand (220-60 cm) with low contents of water, organics, and carbonates - typical characteristics of marine originated clastic materials ([21], 2000). In particular, this sand section also shows relatively high values of Cl/Br ratio, an indicator for high salinity [23,54]. Above the sand section, sediments in core SGI-3 become finer and transit into silty sand (60-0 cm) (Fig. 3). The contents of water, organics, and carbonates in this silty sand section increase substantially, while the values of Cl/Br ratio decrease substantially. It is worth noting that two layers of coarse sand sediments (12-17 cm and 20–28 cm) are embedded in the silty sand section (Fig. 3). XRF analysis reveals high values of Ca/Ti ratio in these two sand layers. The Ca/Ti ratio is an indicator for offshore sediments typically associated with hurricane overwash events ([53], 2019). Thus, the two sand layers at 12-17 cm and 20-28 cm in core SGI-3 are likely overwash layers caused by hurricane events.

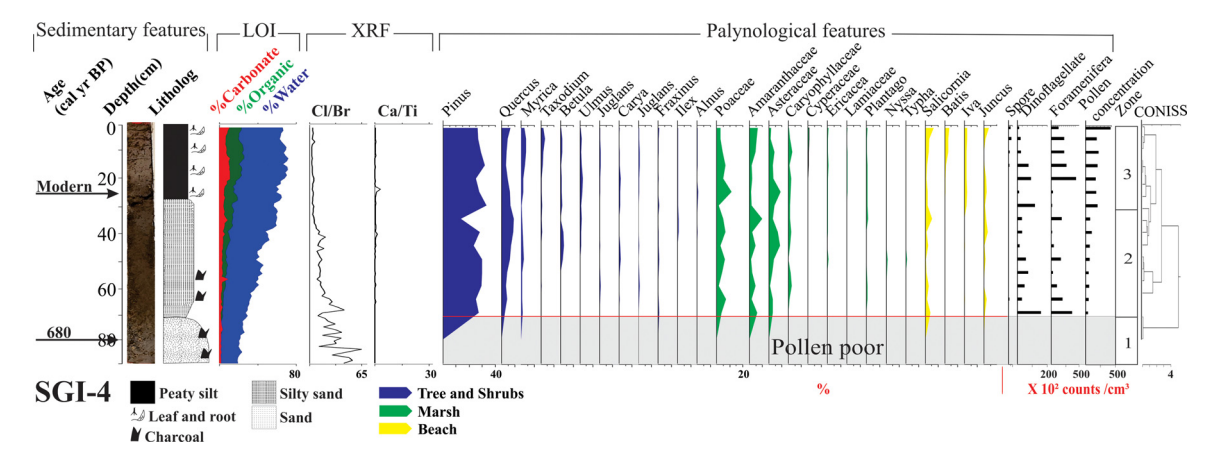


Fig. 4. Multi-proxy results of core SGI-4. Samples from 90 to 70 cm contain less than 50 grains of pollen and non-pollen palynomorphs in total and are marked as "Pollen poor".

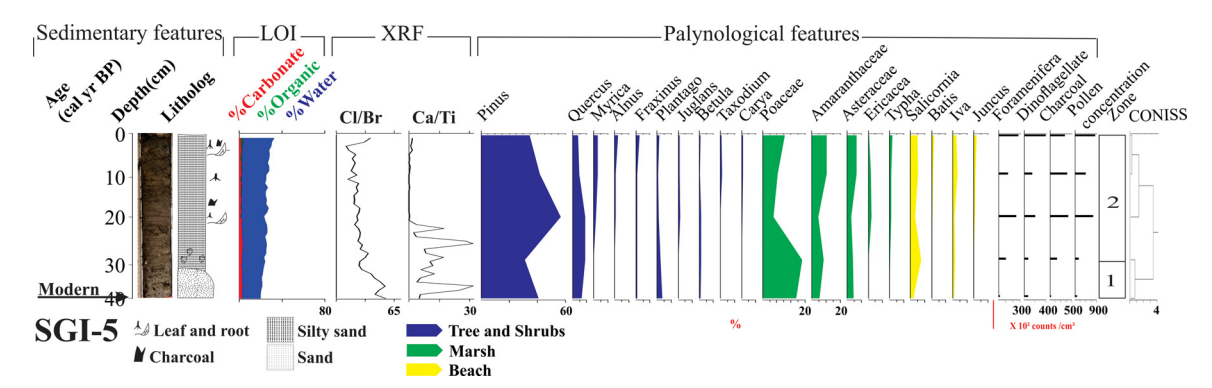


Fig. 5. Multi-proxy results of core SGI-5.

Core SGI-4 is much shorter (90 cm, \sim 800 cal yr BP) and contains three types of sediments. The stepwise decrease of Cl/Br ratios and water content from the sand section (90–70 cm) to the silty sand (70–25 cm) and the peaty silt (25–0 cm) sections exhibit a gradual transition from marine to terrestrial environment from the bottom to the top of the core (Fig. 4). In addition, the Ca/Ti ratios are consistently low throughout the core, suggesting no overwash events were recorded. Moreover, this core was taken from a low-laying marsh behind the mangrove stands. Hence, it contains abundant plant detritus and roots and the highest organic content among the three cores (Fig. 4).

Core SGI-5 (40 cm, <AD1950) is the shortest among the three cores (Fig. 5). Similar to core SGI-4, the values of Cl/Br ratio also gradually decrease from the bottom sand section (40–30 cm) toward the upper silty sand section (30–0 cm), indicating a marine to terrestrial transition. However, high values of Ca/Ti ratio are detected in the bottom half of the core (40–20 cm) (Fig. 5), likely caused by the same overwash events recorded near the top of core SGI-3.

3.3. Palynological data

The pollen percentages, pollen concentrations, and other non-pollen palynomorph results of the three cores are displayed in Figs 3–5. Core SGI-3 is divided into 3 pollen zones, among which, Zone 1 (220–70 cm) is comprised primarily of coarse sand sediments and contains very few grains (< 50 grains in each sample) of pollen and non-pollen palynomorphs (Fig. 3). Since these samples (220–70 cm) contain too few microfossils (<50 grains) to show a meaningful statistical relationship, they are marked as "Pollen poor" in the pollen diagram (Fig. 3). Tree, shrub, and marsh taxa start to appear in Zone 2 (70–25 cm), but at very low concentrations. The pollen assemblages in Zone 2 consist primarily of tree and shrub taxa. Moving toward the core top, pollen concentra-

tions increase significantly in Zone 3 (25–0 cm), and marsh and beach taxa (e.g., Poaceae, *Salicornia*, and *Juncus*) start to consistently appear and become the dominant taxa in the pollen assemblage. In addition, concentrations of foraminifera linings increase substantially in Zone 3, indicating the abundance of these microorganisms. Thus, the transition from Zone 2 to Zone 3 likely indicates the formation of the modern vegetation at the coring site, a coastal marsh comprised of *Juncus, Salicornia*, and *Spartina sp.*. However, no pollen of any mangrove species is found in Zone 3 and throughout core SGI-3 (Fig. 3).

The pollen signature of core SGI-4 highly resembles that of core SGI-3 (Fig. 4). From the bottom to the top of the core, the pollen assemblages exhibit a transition from a pollen barren section (Zone 1, 90–70 cm) to a tree and shrub section (Zone 2, 70–30 cm), and then to a section with abundant beach taxa (Zone 3, 30–0 cm). Similar to core SGI-3, no mangrove pollen are found throughout core SGI-4 (Fig. 4).

Core SGI-5 is divided into 2 pollen zones and the pollen assemblages exhibit relatively less variability throughout the core (Fig. 5). Pollen signature of Zone 1 (40–30 cm) resembles those in cores SGI-4 & 3, a barren section with very few pollen and non-pollen palynomorphs. In Zone 2 (30–0 cm), concentrations of pollen, charcoal, dinoflagellate tests, and foraminifera linings increase significantly, and the pollen assemblage is dominated by trees and shrubs with abundant beach taxa. More importantly, mangrove pollen remains absent in this core (Fig. 5).

3.4. Climatic and environmental record

From 1990 to 2020, meteorological stations near Apalachicola recorded an increasing trend in winter air temperature and RSL, and no significant long-term trend is observed from the precipitation record (Fig. 6). The average WDMAT (1992–2019), WMAAT (1992–2019), MAP (1992–2019), and RSL trend (1990–2020) at Apalachicola are

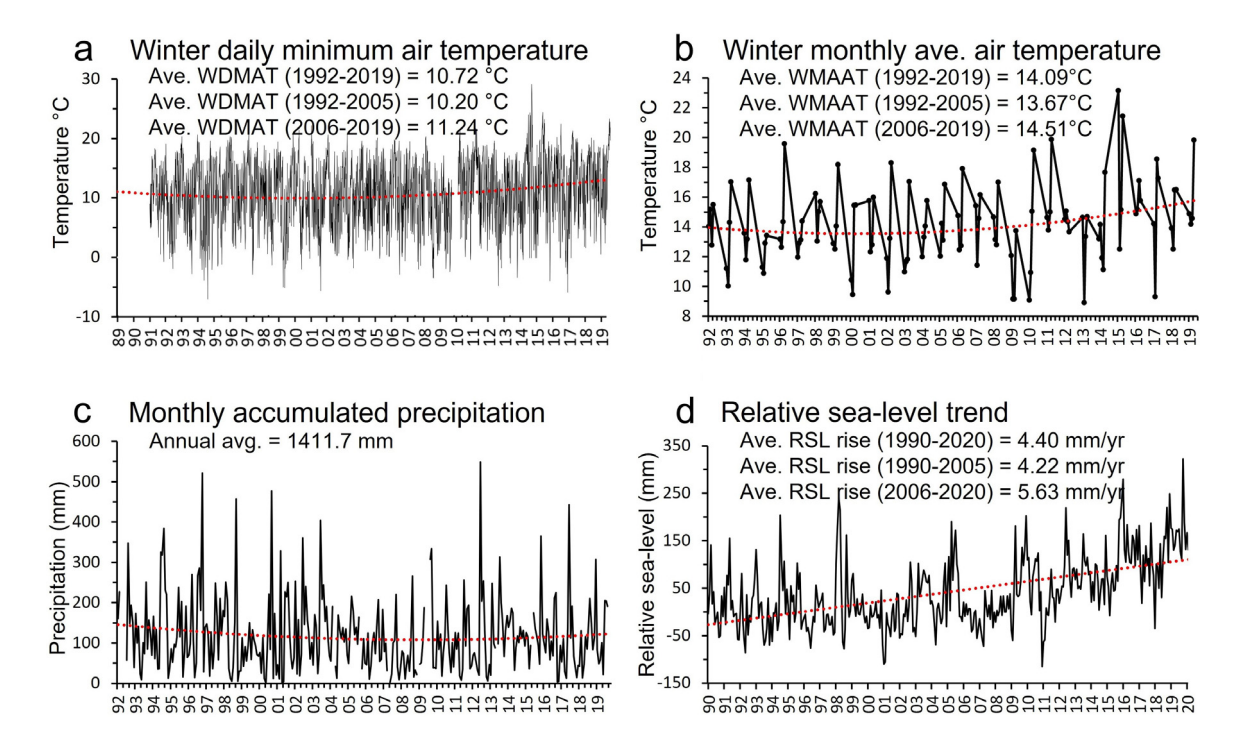


Fig. 6. Meteorological data showing the winter (Dec-Feb) daily minimum air temperature (WDMAT) (1992–2019) (a), winter (Dec-Feb) monthly average air temperature (WMAAT) (1992–2019) (b), monthly accumulated precipitation (MAP) (1992–2019) (c), and RSL trends (190–2020) (d) from meteorological stations near Apalachicola.

10.72 °C, 14.09 °C, 1411.7 mm, and 4.4 mm/yr, respectively. Using 2005 as the median to split the dataset, the average WDMAT of the earlier (1992–2005) and recent halves (2006–2019) are 10.2 °C and 11.24 °C, the average WMAAT of the earlier (1992–2005) and recent halves (2006–2019) are 13.67 °C and 14.51 °C, and the rates of RSL rise of the earlier (1990–2005) and recent halves (2006–2020) are 4.22 and 5.63 mm/yr, respectively (Fig. 6).

4. Discussion

4.1. Late-Holocene vegetation dynamics and coastal geomorphological development

Our paleoenvironmental record reveals a comprehensive history of coastal vegetation and sediment morphology of St. George Island, Apalachicola for the last 1500 years (Figs. 3-5). Overall, the multi-proxy dataset of cores SGI-3, SGI-4, and SGI-5 shows a clear history of marine progradation since at least 1490 cal yr BP (Fig. 3). The bottom sections in SGI-3 and SGI-4 (Zone 1, ~1490-650 cal yr BP) are comprised of mostly sand that contains few pollen and non-pollen palynomorphs (<50 grains). Moreover, these sand sections are also characterized by high Cl/Br ratios - an indicator for high salinity [23,52]. Thus, these data suggest that our study area was in a subtidal sandy environmental where the hydrodynamics was too strong for the deposition or preservation of microfossils. We believe this stage likely represents the precursor of St. George Island, a submerged marine environment before the barrier island was formed, hence the high salinity. This pollen-poor section also suggests that no subaerial vegetation was established in the vicinity of our study area during the period between ~1490 and 650 cal yr BP (Zone 1 in SGI-3&4).

Above the pollen-poor sections, arboreal pollen types (e.g., *Pinus* and *Quercus*) and herbs (e.g., Poaceae and Amaranthaceae) start to appear in Zone 2 of core SGI-3 and SGI-4 and in Zone 1 of core SGI-5 (Figs. 3, 4), albeit still in low concentrations (Fig. 5). This pollen assemblage resembles that of the mudflats found across the GOM coastlines today (Yao et al., [37,36]). In addition, sediments in these sections also tran-

sition from sand to finer silty sand. Such vegetation and sedimentary transformation indicate the formation of the barrier island and development of mudflats on the bayside of St. George Island since ~650 cal yr BP, likely facilitated by the stabilization of RSL in the Late-Holocene [9] and the longshore currents that transported sediments from the east. The growth and expansion of vegetation on the mudflats in term trapped more fine-grain sediments that changed the sediment composition at the study area.

Moving to the top part of the cores (Zone 3 in SGI-3&4 and Zone 2 in SGI-5), a drop of the Cl/Br ratios indicates a decline in salinity. This change was probably caused by the continuation of shoreline progradation on the barrier island and vertical sediment accumulation in the study area, as registered by a decrease of marine signals in all the cores (Figs. 3–5). In addition, the organic contents and concentrations of pollen and foraminifera also increase in all three cores, indicating the flourishing of vegetation and microorganism. This transition marks the formation of the modern coastal marshes on the bayside of St. George Island (Fig. 2). The "modern" radiocarbon dates at 40 cm in core SGI-5 and 25 cm in core SGI-4 (Table 1) suggest that the coastal marshes started to flourish at our study area since the 1950s, facilitated by the stabilization of the barrier island on its bayside.

Interestingly, although field surveys show that *A. germinans* and *R. mangle* populations have expanded in recent years [40], no pollen of either mangrove species were found throughout cores SGI-3, SGI-4, and SGI-5. We think this paradox suggests that the mangrove colonies on St. George Island were formed only during the most recent decades, so that the individual trees are young and short in stature. Field observations showed that the red and black mangroves at our study sites were short with a shrubby growth form and consistent with a young, pioneering population (Fig. S1 in the Supplementary Content). It is typical that mangrove would not have been registered in the pollen record before a mature mangrove forest has been formed, resulting in a decade or so of time lag in the pollen record [44,52]. Thus, we think this discrepancy is due to the time lag reflected in the pollen record. In addition, the bottom sections of core SGI-3 and SGI-4 represent an offshore subtidal sandy environment between ~1490 and 800 cal yr BP (Figs. 3, 4). Our data sug-

gest that St. George Island had not been formed until ~800 cal yr BP, making it unlikely for mangroves to establish prior to that. More importantly, some mangroves, at least R. mangle, are prolific pollen producers, and their pollen can be dispersed widely by wind and currents [47]. If mature mangrove stands have ever formed in the vicinity of the St. George Island during the Late-Holocene, their pollen would have been registered in the sediment profiles, even in the "Pollen poor" sections in core SGI-3 and SGI-4. However, not a single mangrove pollen grain was found throughout all three cores. Moreover, studies from Florida show that sediment profiles in mature mangrove stands contain up to 50% (dry weight) of organic content due to rapid belowground peataccumulation by mangroves [50,52]. In comparison, the organic contents in the inferred marine, mudflat, and coastal marsh stages in our study area are <2%, 2–10%, and 10–20%, respectively (Figs. 3–5). Thus, it is reasonable to conclude that mature mangrove stands have never been established in our study area on St. George Island until the most recent decades. Although historical documents have recorded mangrove sightings since the mid-19th century [40], we believe they spotted only a few individuals of mangroves that quickly died out, instead of mature mangrove colonies.

In sum, the multi-proxy dataset recorded a gradual formation and expansion of St. George Island since the Late-Holocene. No mangrove pollen and mangrove peat are found in the cores since ~1490 cal yr BP (Fig. 3). Thus, the current mangrove encroachment at St. George Island is caused by the recent climate warming instead of a recurring phenomenon tied with past global climate variability. However, we acknowledge that it is possible that other mangrove colonies near the Apalachicola Bay, especially the ones on Dog Island (Fig. 1), could have been established for a longer period than that was documented on St. George Island. Future studies are needed to explore the late-Holocene histories of other large mangrove colonies around the Apalachicola Bay and along the Gulf of Mexico coast.

4.2. Inferred driving factors behind mangrove tropicalization

Although we do not totally disregard the possibility that mangroves could have colonized the Apalachicola Bay prior to the 21st century, field surveys and our multi-proxy data indicate that mangrove expansion only occurred during the most recent decades (Fig. 1) [40]. We believe the accelerated global warming in the 21st century was driving the mangrove poleward migration and expansion at Apalachicola, the current mangrove boreal range limit along the GOM (Fig. 6).

Previous studies have documented poleward mangrove expansions at their boreal and austral range limits around the globe in the recent decades (e.g. [4,38,32]). These mangrove expansions are attributed to factors such as RSL rise, warming winter, and precipitation, on a global scale (Blasco et al., [30,31,39]). Moreover, the factors governing the range and distribution of mangroves have been attributed to sealevel and temperature (air and sea surface) on the millennial time-scale [6,10,3,13,2,52], and to local factors such as tidal activities, hurricanes, delta switching, and morphological change on centennial to decadal time-scales ([27,56]).

In the case of Apalachicola, our decadal climatic and environmental record shows a trend of rising winter minimum and average air temperature and RSL since the 1990s, whereas no obvious trend is observed in precipitation (Fig. 6). In particular, using 2005 as the median for all metrics, the winter minimum air temperature (WDMAT) and winter average air temperature (WMAAT) are both ~1 °C warmer, and the rate of RSL rise is 1.41 mm/yr faster (accelerated by ~33.4% than the period between 1990 and 2005) during the period between 2006 and 2019 (Fig. 6). These data support our theory that the mangrove expansion at Apalachicola is likely tied with accelerated climate warming during the recent decades. More importantly, the climatic record shows that the winter minimum air temperature has risen for over 1 °C at Apalachicola between 2006 and 2019, coinciding with the most plausible timeline of mangrove colonization (2004–2009) at the same area [57]. Thus, it is

likely that the warmer winters played an important role in the mangrove expansion at Apalachicola. This finding is in line with the previous discovery that winter freeze events are the primary threshold controlling the range of mangroves in North America (Cavanagh et al., [32,40]). In addition, although the RSL was rising at 4.4 mm/yr after 1990 and accelerated to 5.63 mm/yr from 2006 to 2020 (Fig. 6d), it did not impact mangrove colonization on St. George Island. This result is also in line with the latest discovery of a RSL threshold at 0.61 cm/yr, above which the RSL rise will inhibit the growth of mangrove colonies [39]. It is reasonable to believe that while the RSL is rising at a rapid but tolerable pace (for mangroves) at 5.63 mm/yr, it gave mangroves the advantage to out-compete other graminoids and succulent plants that grow on similar terrains on the bayside of St. George Island. As for precipitation, the average annual accumulated precipitation at Apalachicola was 1411.7 mm/yr between 1992 and 2019, much higher than the threshold (780 mm/y) that will dampen the mangrove vitality along the GOM [30,31]. Thus, precipitation likely did not play an important role on the mangrove dynamics at Apalachicola. Overall, our record suggests that the rising winter temperature, especially the winter minimum air temperature, and RSL rise are the most probable causes for mangrove expansion at St. George Island, Apalachicola during the recent decades.

5. Conclusion

This paper presents one of the first studies that documented the long-term vegetation dynamics and coastal morphological changes at Apalachicola, the mangrove boreal range limit along the GOM, from the Late-Holocene. Our data suggest that the current mangrove expansion on St. George Island has only started during the recent decades, and it is not a recurring phenomenon driven by Late-Holocene climatic variations. Under the predicted warming trend and continuous RSL rise in the 21st century (IPCC, 2021), it is likely that mangrove encroachment into coastal marshes will accelerate at Apalachicola and other areas near their poleward range limits. Our multi-proxy record and climatic data indicate that the mangrove expansion on St. George Island during the recent decades is facilitated by the warming winter and a RSL rise rate that is rapid but not intolerable by mangroves [39]. The two main limitations of this study are: (1) While we focus on macro-climatic factors, many other regional- and local-factors such as tides, hurricanes, topography, and plant physiology may also influence the mangrove dynamics [42,26,24,16,32,7]. (2) It is possible that other localities around the Apalachicola Bay might have harbored mangroves for a longer period than we documented. More studies are needed to reveal the impacts of regional and local factors on poleward mangrove expansion and to document the mangrove history at other larger colonies near their boreal range limits.

Declaration of Competing Interest

The authors declare that they have no known competing financial interests or personal relationships that could have appeared to influence the work reported in this paper.

Acknowledgements

We thank Apalachicola National Estuarine Research Reserve for their logistic support before and during the field sample collection. This research was supported by grants from the U.S. National Science Foundation (Grant # GSS-1759715).

Author contributions

Qiang Yao conceived the hypothesis, led the sample collection, and wrote the paper. Erika Rodrigues led the multi-proxy analysis, contributed to writing and editing, and assisted in the fieldwork and vegetation survey. Kam-biu Liu directed the project and fieldwork and con-

tributed to writing, editing, and data interpretation. Marcelo Cohen contributed to remote sensing analysis. Caitlin Snyder assisted in field sampling. Nicholas Culligan assisted in laboratory analysis.

Data availability

All of the datasets produced in this article will be available to share from the corresponding author upon request, once this manuscript is accepted for publication.

Supplementary materials

Supplementary material associated with this article can be found, in the online version, at doi:10.1016/j.ecochg.2022.100056.

References

- D.M. Alongi, Present state and future of the world's mangrove forests, Environ. Conserv. 29 (03) (2002) 331–349.
- [2] D.M. Alongi, Mangrove forests: resilience, protection from tsunamis, and responses to global climate change, Estuar. Coast. Shelf Sci. 76 (2008) 1–13, doi:10.1016/j.ecss.2007.08.024.
- [3] F. Blasco, Mangroves as indicators of coastal change, Catena 27 (1996) 167–178.
- [4] K.C. Cavanaugh, J.R. Kellner, A.J. Forde, D.S. Gruner, J.D. Parker, W. Rodriguez, I.C. Feller, Poleward expansion of mangroves is a threshold response to decreased frequency of extreme cold events, Proc. Natl. Acad. Sci. 111 (2) (2014) 723–727.
- [5] K.C. Cavanaugh, E.M. Dangremond, C.L. Doughty, A. Park Williams, J.D. Parker, M.A. Hayes, W. Rodriguez, I.C. Feller, Climate-driven regime shifts in a mangrovesalt marsh ecotone over the past 250 years, Proc. Natl. Acad. Sci. U. S. A. 116 (2019) 21602–21608, doi:10.1073/pnas.1902181116.
- [6] V.J. Chapman, Mangrove biogeography, in: G.E. Walsh, S.C. Snedaker, H.J. Teas (Eds.), International Symposium on Biology and Management of Mangroves Eds., University of Florida Press, Miami, 1975 pp. 179–212.
- [7] Cohen, M.C.L., Souza, A.V.de, Liu, K.B., Rodrigues, E., Yao, Q., Pessenda, L.C.R., Rossetti, D., Ryu, J., Dietz, M., 2021. Effects of beach nourishment project on coastal geomorphology and mangrove dynamics in Southern Louisiana, USA. Remote Sens.. 13, 2688. 10.3390/RS13142688
- [8] R.S. Comeaux, M.A. Allison, T.S. Bianchi, Mangrove expansion in the Gulf of Mexico with climate change: implications for wetland health and resistance to rising sea levels, Estuar. Coast. Shelf Sci. 96 (2012) 81–95.
- [9] J.F. Donoghue, Sea level history of the northern Gulf of Mexico coast and sea level rise scenarios for the near future, Clim. Chang. 107 (2011) 17–33, doi:10.1007/s10584-011-0077-x.
- [10] N.C. Duke, Mangrove Floristics and Biogeography, American Geophysical Union (AGU), 1992 pp. 63–100, doi:10.1029/CE041p0063.
- [11] K.C. Ewel, R.R. Twilley, J.E. Ong, Different kinds of mangrove forests provide different goods and services, Glob. Ecol. Biogeogr. Lett. 7 (1998) 83–94.
- [12] Food and Agriculture Organization (FAO) of the United NationsThe World's Mangroves, 1980–2005: A Thematic Study in the Framework of the Global Forest Resources Assessment 2005, Food and Agriculture Organization of the United Nations, 2007.
- [13] F. Fromard, C. Vega, C. Proisy, Half a century of dynamic coastal change affecting mangrove shorelines of French Guiana. A case study based on remote sensing data analyses and field surveys, Mar. Geol. 208 (2004) 265–280, doi:10.1016/j.margeo.2004.04.018.
- [14] C. Giri, J. Long, Mangrove reemergence in the northernmost range limit of eastern Florida, Proc. Natl. Acad. Sci. U. S. A. 111 (15) (2014) E1447-E1448.
- [15] E. Grimm, TILIA and TILIAGRAPH: PC Spreadsheet and Graphic Software For Pollen Data, INQUA Sub-Commission on Data-Handling Methods Newsletter, 1990.
- [16] H. Guo, Y. Zhang, Z. Lan, S.C. Pennings, Biotic interactions mediate the expansion of black mangrove (A vicennia germinans) into salt marshes under climate change, Glob. Chang. Biol. 19 (9) (2013) 2765–2774.
- [17] H. Guo, C. Weaver, S.P. Charles, A. Whitt, S. Dastidar, P. D'Odorico, J.D. Fuentes, J.S. Kominoski, A.R. Armitage, S.C. Pennings, Coastal regime shifts: rapid responses of coastal wetlands to changes in mangrove cover, Ecology 98 (3) (2017) 762–772.
- [18] C.W. Harper, Facies Models revisited: An examination of Quantitative Methods, Geoscience Canada, 1984.
- [19] J.J. Kelleway, K. Cavanaugh, K. Rogers, I.C. Feller, E. Ens, C. Doughty, N. Saintilan, Review of the ecosystem service implications of mangrove encroachment into salt marshes, Glob. Chang. Biol. 23 (10) (2017) 3967–3983.
- [20] Little, E.L. 1978. Atlas of United States trees. Volume 5. Florida. Miscelleneous Publication No. 1361. Washington D.C.: U.S. Department of Agriculture Forest Service.
- [21] K.B. Liu, M.L. Fearn, Lake-sediment record of late Holocene hurricane activities from coastal Alabama, Geology 21 (9) (1993) 793–796.
- [22] K.B. Liu, M.L. Fearn, Reconstruction of prehistoric landfall frequencies of catastrophic hurricanes in Northwestern Florida from lake sediment records, Quat. Res. 54 (2) (2000) 238–245.
- [23] K.B. Liu, T.A. McCloskey, T.A. Bianchette, G. Keller, N.S. Lam, J.E. Cable, J. Arriola, Hurricane Isaac storm surge deposition in a coastal wetland along Lake Pontchartrain, southern Louisiana, J. Coast. Res. (2014) 266–271 (70 (10070)).

- [24] X. López-Medellín, E. Ezcurra, C. González-Abraham, J. Hak, L.S. Santiago, J.O. Sickman, Oceanographic anomalies and sea-level rise drive mangroves inland in the Pacific coast of Mexico, J. Veg. Sci. 22 (1) (2011) 143–151.
- [25] Michot, T.C., Day, R.H., and Wells, C.J., 2010. Increase in black mangrove abundance in coastal Louisiana. Louisiana Natural Resources News (Newsletter of the La. Assoc. of Professional Biologists), January 2010: 4–5.
- [26] Pages 96–123 P.A. Montagna, J. Brenner, J. Gibeaut, S. Morehead, J. Schmandt, G.R. North, J. Clarkson, Coastal impacts, The Impact of Global Warming On Texas, editors University of Texas Press, Austin, Texas, USA, 2011. Second edition.
- [27] C.A. Moraes, N.A. Fontes, M.C. Cohen, M.C. França, L.C. Pessenda, D.F. Rossetti, M.I. Francisquini, J.A. Bendassolli, K. Macario, Late Holocene mangrove dynamics dominated by autogenic processes, Earth Surf. Process. Landforms. (2017), doi:10.1002/esp.4167.
- [28] Odum, W.E., McIvor, C.C., and Smith, J.T., 1982. The ecology of mangroves in south Florida: a community profile. US Fish and Wildlife Service, Office of Biological Services, Washington, D.C. FWS/OBS-81-24. 144 pp.
- [29] M.J. Osland, N. Enwright, R.H. Day, T.W. Doyle, Winter climate change and coastal wetland foundation species: salt marshes vs. mangrove forests in the southeastern United States, Glob. Chang. Biol. 19 (5) (2013) 1482–1494.
- [30] M.J. Osland, N.M. Enwright, R.H. Day, C.A. Gabler, C.L. Stagg, J.B. Grace, Beyond just sea-level rise: considering macroclimatic drivers within coastal wetland vulnerability assessments to climate change, Glob. Chang. Biol. 22 (1) (2016) 1–11.
- [31] M. Osland, L.C. Feher, K.T. Griffith, K.C. Cavanaugh, N.M. Enwright, R.H. Day, C.L. Stagg, K.W. Krauss, R.J. Howard, J.B. Grace, K. Rogers, Climatic controls on the global distribution, abundance, and species richness of mangrove forests, Ecol. Monogr. 87 (2) (2017) 341–359.
- [32] M.J. Osland, R.H. Day, C.T. Hall, L.C. Feher, A.R. Armitage, J. Cebrian, K.H. Dunton, A.R. Hughes, D.A. Kaplan, A.K. Langston, A. Macy, Temperature thresholds for black mangrove (Avicennia germinans) freeze damage, mortality and recovery in North America: refining tipping points for range expansion in a warming climate, J. Ecol. 108 (2) (2020) 654–665.
- [33] M.J. Osland, P.W. Stevens, M.M. Lamont, R.C. Brusca, K.M. Hart, J.H. Waddle, C.A. Langtimm, C.M. Williams, B.D. Keim, A.J. Terando, E.A. Reyier, Tropicalization of temperate ecosystems in North America: the northward range expansion of tropical organisms in response to warming winter temperatures, Glob. Chang. Biol. 27 (13) (2021) 3009–3034.
- [34] R. Core Team, R: A Language and Environment for Statistical Computing, (R Foundation for Statistical Computing, Vienna), 2013.
- [35] R. Ribeiro, A. de, A.S. Rovai, R.R. Twilley, E. Castañeda-Moya, Spatial variability of mangrove primary productivity in the neotropics, Ecosphere 10 (2019), doi:10.1002/ecs2.2841.
- [36] J. Ryu, K.B. Liu, T.A. Bianchette, T. McCloskey, Identifying Forcing Agents of Environmental Change and Ecological Response On the Mississippi River Delta, Southeastern Louisiana. Science of The Total Environment, 2021 p.148730.
- [37] E. Rodrigues, M.C.L. Cohen, K. Liu, L.C.R. Pessenda, Q. Yao, J. Ryu, D. Rossetti, A. de Souza, M. Dietz, The effect of global warming on the establishment of mangroves in coastal Louisiana during the Holocene, Geomorphology 381 (2021) 107648, doi:10.1016/j.geomorph.2021.107648.
- [38] N. Saintilan, N.C. Wilson, K. Rogers, A. Rajkaran, K.W. Krauss, Mangrove expansion and salt marsh decline at mangrove poleward limits, Glob. Chang. Biol. 20 (1) (2014) 147–157.
- [39] N. Saintilan, N.S. Khan, E. Ashe, J.J. Kelleway, K. Rogers, C.D. Woodroffe, B.P. Horton, Thresholds of mangrove survival under rapid sea level rise, Science 368 (6495) (2020) 1118–1121
- [40] C.M. Snyder, L.C. Feher, M.J. Osland, C.J. Miller, A.R. Hughes, K.L. Cummins, in: The Distribution and Structure of Mangroves (Avicennia germinans and Rhizophora mangle) Near a Rapidly Changing Range Limit in the Northeastern Gulf of Mexico, Estuaries and Coasts, 2021, pp. 1–15.
- [41] Stuiver, M., Reimer, P.J., Reimer, R., 2021. CALIB radiocarbon calibration 8.2. URL http://calib.org/calib/calib.html (accessed 3.31.21).
- [42] M.L.G. Soares, G.C.D. Estrada, V. Fernandez, M.M.P. Tognella, Southern limit of the Western South Atlantic mangroves: assessment of the potential effects of global warming from a biogeographical perspective, Estuar. Coast. Shelf Sci. 101 (2012) 44–53.
- [43] P. Taillardat, D.A. Friess, M. Lupascu, Mangrove blue carbon strategies for climate change mitigation are most effective at the national scale, Biol. Lett. 14 (2018) 20180251, doi:10.1098/rsbl.2018.0251.
- [44] L.E. Urrego, C. González, G. Urán, J. Polanía, Modern pollen rain in mangroves from San Andres Island, Colombian Caribbean, Rev. Palaeobot. Palynol. 162 (2) (2010) 168–182.
- [45] M.J. Williams, Native Plants for Coastal Restoration: What, When, and How for Florida, USDA, NRCS, Brooksville Plant Materials Center, Brooksville, FL, 2007 51p.
- [46] Walker, R.G., 1992. Facies, facies models and modern stratigraphic concepts. In: Walker, R.G., James, N.P. (Eds.), Facies Models - Response to Sea Level Change. Geological Association of Canada, Newfoundland.
- [47] C. Weng, M.B. Bush, M.R. Silman, An analysis of modern pollen rain on an elevational gradient in southern Peru, J. Trop. Ecol. 20 (2004) 113–124, doi:10.1017/S0266467403001068.
- [48] D.A. Willard, C.E. Bernhardt, L. Weimer, S.R. Cooper, D. Gamez, J. Jensen, Atlas of pollen and spores of the Florida everglades, Palynology 28 (2004) 175–227.
- [49] R.P. Wunderlin, B.F. Hansen, Atlas of Florida vascular plants. [SM Landry and KN Campbell (Application development), Florida Center For Community Design and Research.]. Institute for Systematic Botany, University of South Florida, Tampa, FL, 2008 http://www.florida.plantatlas.usf.edu. Accessed: September 2021. 11:2011.

- [50] Q. Yao, K.B. Liu, W.J. Platt, V.H. Rivera-Monroy, Palynological reconstruction of environmental changes in coastal wetlands of the Florida Everglades since the mid-Holocene, Quat. Res. 83 (3) (2015) 449–458.
- [51] Q. Yao, K.B Liu, Changes in modern pollen assemblages and soil geochemistry along coastal environmental gradients in the coastal Everglades of South Florida, Front. Ecol. Evol. 5 (2018) 178.
- [52] Q. Yao, K.B. Liu, Dynamics of marsh-mangrove ecotone since the mid-Holocene: a palynological study of mangrove encroachment and sea level rise in the Shark River Estuary, Florida, PLoS ONE 12 (3) (2017) e0173670.
- [53] Q. Yao, K.B. Liu, J. Ryu, Multi-proxy characterization of Hurricanes Rita and Ike storm deposits in the Rockefeller Wildlife Refuge, southwestern Louisiana, J. Coast. Res. 85 (2018) 841–845 10085.
- [54] Q. Yao, K.B. Liu, E. Rodrigues, T. Bianchette, A.A. Aragón-Moreno, Z. Zhang, A geochemical record of Late-Holocene hurricane events from the Florida Everglades, Water Resour. Res. 56 (8) (2020) e2019WR026857.
- [55] Q. Yao, K.B. Liu, Y. Wu, A.A. Aragón-Moreno, E. Rodrigues, M. Cohen, A.V. de Souza, L.M. Farfán, J.L. Antinao, A multi-proxy record of hurricanes, tsunami, and post-disturbance ecosystem changes from coastal southern Baja California, Sci. Total Environ. 796 (2021) 149011.
- [56] S.R. Ribeiro, E.J.L. Batista, M.C. Cohen, M.C. França, L.C. Pessenda, N.A. Fontes, I.C. Alves, J.A. Bendassolli, Allogenic and autogenic effects on mangrove dynamics from the Ceará Mirim River, north-eastern Brazil, during the middle and late Holocene, Earth Surface Processes and Landforms 43 (8) (2018) 1622–1635.
- [57] C.M. Snyder, L.C. Feher, M.J. Osland, C.J. Miller, A.R. Hughes, K.L. Cummins, The distribution and structure of mangroves (Avicennia germinans and Rhizophora mangle) near a rapidly changing range limit in the Northeastern Gulf of Mexico, Estuaries and Coasts 45 (1) (2022) 181–195.